Multi-phase Navier-Stokes FE solver with Level set description and X-FEM

By
Elham Maghsoudi

A thesis presented to
Universitat Politècnica de Catalunya (UPC)
joint with
Swansea University
in fulfilment of the
thesis requirement for the degree of
Master of Applied Science
in
Computational Mechanics
Supervisor: Pedro Diez

Contents

1 Introduction 2

2 Problem Statement of Navier Stokes Equation 6
- 2.1 Strong Form . . . 6
- 2.2 Finite Element Formulation . . . 7

3 Multiphase Flow 11
- 3.1 Numerical Difficulties . . . 11
- 3.2 Numerical Methods for Modelling Interface . . . 12
- 3.3 The Level Set Method . . . 12
- 3.4 Space discretization . . . 16
- 3.5 Time discretization . . . 16
- 3.6 Enriched Solution (XFEM) . . . 18

4 GLS Stabilization 21
- 4.1 GLS Formulation of Navier Stokes Equation . . . 21
- 4.2 Extra Stablized Matrices . . . 24
- 4.3 GLS Stabilization Factor . . . 25

5 Results 27
- 5.1 Rayleigh-Taylor Instability . . . 27
- 5.2 Convergence criteria . . . 27
- 5.3 Transient Navier Stokes without enrichment . . . 28
- 5.4 Volume conservation . . . 30
- 5.5 Lack of Symmetry . . . 30

6 Conclusion 37

Abstract

Transient Navier Stokes equation has been solved numerically using FEM (Finite Elements Method). In order to model different phases, level set method is used and enrichment is added to increase the accuracy. Rayleigh-Taylor Instability is used as a bench mark to verify the code which has been implemented in MATLAB. The results obtained from Transient Navier Stokes equation without enrichment are in good agreement with obtained results from other numerical simulations. Although elimination of surface tension affects the results specially in the case that stabilization has not been applied, eddies have been observed in some values of viscosities in Rayleigh-Taylor Instability which is a result of Using stable mini element.

The accuracy has been defined based on conservation equation, using an error which is calculated along time stepping procedure to calculate volume changes. This error is acceptably low and decreases by mesh refinement.

Acknowlegments

I would like to deeply appreciate my supervisor, Professor Pedro Diez, for his patience, guidance and help. Working with him had been an inspiring experience. I want to express my appreciation to Esther Sala Lardies for patiently answering my questions. I also thank Sergio Zlotnik for his encouragement and introducing appropriate resources in this research.

I would like to thank European commission joint with CIMNE for financial supports during these 2 years. I would also like to thank Swansea University and UPC faculty members and staff specially Lelia Zielonka and Mr. Gaskin for their help and supports.

Furthermore, my thanks go to whom never let me far from family and country; Blanca Pascual Oliver, Laurence Grosjean, Tahereh Melksari and Somayeh Heidarvand; also my friends: Lindaura Steffens, Giorgio Giorgiani, Katia Gualtieri, Luis Pedro Montejano, Cesar Davalos Chargoy, Yasamin Akabarieh, Asal Mahdavi, Mahdieh Motamedi and Ani Jamgochian.

Above all, I want to express my gratitude to my family, my parents, Farzaneh and Mohamad, and my brothers, Amir and Arash, for their care and endless love. This work is dedicated to them.

Chapter 1

Introduction

Many practical applications in Computational Mechanics require solving numerically the Navier-Stokes equations for a multiphase flow. It can be applicable in many cases such as free surface flows which feature in marine engineering and are characterized by wind-water interactions and unsteady waves, jet flows, bubble dynamics and liquid film flows. Hence, it can be applied in a various range of industrial cases from optimization the design of ships, submarines and liquid tanks, design of engines in combustion view, and also design of coating and drying processes in the case of polymer production [1].

This work aims at solving a two-phase Navier-Stokes flow for two immiscible materials. There are some difficulties in solving Navier stokes equations for two phase case. The first one is that it is possible to model the fluid using Eulerian description but we will confront problems along the interfaces. Other difficulties arise from nonlinear convective terms and unsteady term appearing in the equations.

Navier-Stokes equations are governing equations of the problem which can be solved analytically in simple cases but numerical techniques are required to obtain the approximations in general cases.

The technique which is used in this thesis to approximate solutions of partial differential equations, as the Navier-Stokes, is the Finite Element Method (FEM). It is based on a variational or weak statement of the problem and a discretization of the variational equations. The FEM is generally attractive because it is robust, flexible in its ability to model complex geometry, algorithmically modular, and mathematically very well understood. The FEM has a long history in geodynamics, predominantly because of its ability to accurately solve problems with strong gradients [2], but also

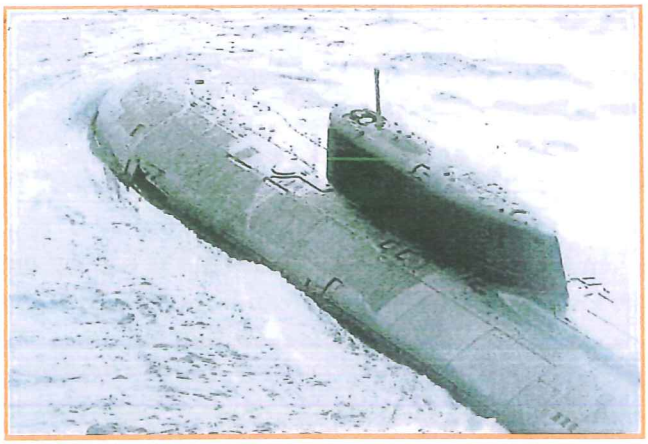

Figure 1.1: Flow around submarine

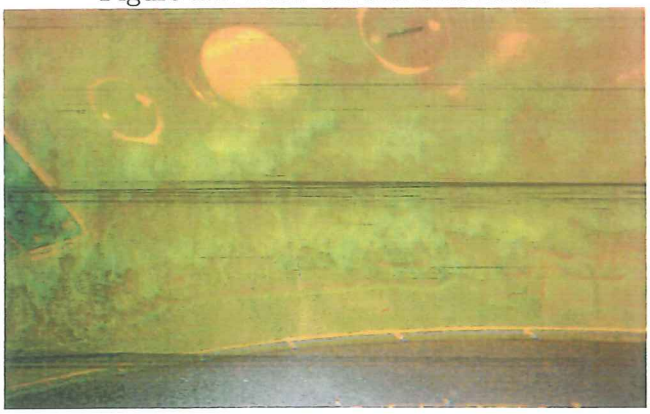

Figure 1.2: Bubbly flow

Figure 1.3: Jet flow

because its geometrical flexibility; it allows for modelling spherical and cartesian domains without reformulating the equations in spherical coordinates. Adopting the FEM as the basis for the numerical solution allows dealing with material properties with steep variations (large gradients).

Another widely used technique to solve partial differential equations is the Finite Difference method (FD). Both techniques, FEM and FD, are based on a discretization (supported by a mesh) of the simulation domain. FEM uses unstructured meshes allowing for concentrating elements in the regions where more resolution is needed while leaving coarse regions where the solution is simpler or easier to interpolate. As the standard version of FD requires using structured meshes, it is difficult to control the resolution in different regions of the domain. Moreover, curved boundaries and boundaries not parallel to the cartesian axis are difficult to handle with FD while it is straightforward with FEM.

The mechanical flow problem based on Navier-Stokes equations is solved by a mixed Finite Element Method with both velocity and pressure unknowns. Its multiphase character is handled by a level set technique. The level set approach is a computationally efficient way of tracking the different materials location. It allows for describing the interface without requiring it to conform with the mesh. A solution with discontinuous gradient on the interface described by the level set is expected. The discontinuity is generated by the jump of material properties across this interface.

Here we enrich the finite element solution allowing for a discontinuous gradient inside the elements crossed by the level set, using a XFEM technique. Classical finite elements cannot handle with such a solution. Moreover, the mechanical problem is nonlinear due to the viscosity dependence on the velocity gradient. We found that a basic Picard method suffices to solve the nonlinear problem up to the accuracy required.

Chapter 2

Problem Statement of Navier Stokes Equation

Strong formulation of unsteady Navier Stoke problem is stated as follows:

2.1 Strong Form

$$v_t - \nu\nabla^2 v + (v \cdot \nabla)v + \nabla p = \rho g \quad \text{in} \quad \Omega\times]0,T[, \tag{2.1}$$

$$\nabla \cdot v = 0 \quad \text{in} \quad \Omega\times]0,T[, \tag{2.2}$$

$$v = v_D \quad \text{on} \quad \Omega_D]0,T[, \tag{2.3}$$

$$-pn + \nu(n \cdot \nabla)v = t \quad \text{on} \quad \Omega_N]0,T[, \tag{2.4}$$

$$v(x,0) = v_0(x) \quad \text{in} \quad \Omega. \tag{2.5}$$

ρg is representive of body force, v_D, prescribed velocities on portion Γ_D of the boundary and imposed boundary tractions t on the remaining portion Γ_N. v and p are the velocity and pressure field respectively.

Equation 2.2 is governing equation of mass conservation. The problem must be completed with suitable boundary conditions. Typically the velocity v_D is prescribed

on a portion Γ_D of the boundary (Equation 2.3).

A boundary traction t has been imposed on the complementary portion Γ_N as Equation 2.4. Where vector n denotes the unit outerward normal to the boundary. The initial value of the velocity field at the initial time $t = 0$ is given in Ω as described in Equation 2.5.

Since no time derivative of pressure appears in governing equations, no initial condition is specified for the pressure. Pressure is only presented by its gradient in the Navier Stokes equations in contrary of velocity which is imposed eveywhere on the boundary Γ. Thus, the pressure is determined only up to an arbitrary constant.

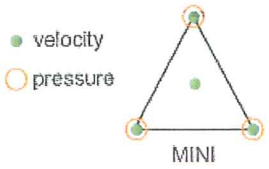

Figure 2.1: Mini Element

The variable formulation with both velocity and pressure unknowns, leads to the so-called mixed finite elements. Such methods present numerical difficulties caused by the saddle point nature of the resulting variational problem. The algebraic system for the nodal values of velocity and pressure in a Galerkin formulation is governed by a partitioned matrix with a null sub matrix on the diagonal. Solvability of such a system depends on a proper choice of finite element spaces for velocity and pressure interpolation. In this work the wellknown minielement is used (Fig.2.1). This triangular element is composed by three pressure nodes at the vertices (linearly interpolated) and four velocity nodes (three linear nodes at the vertices and one central quadratic node). The minielement satisfy the LBB compatibility condition ([3], [4] and [5]) which guarantees the solvability of the system.

2.2 Finite Element Formulation

The formulation of the weak peroblem requires the following condition is satisfied

which means a function u is square-integrable on a domain Ω:

$$\int_{\Omega} u^2 d\Omega \leq \infty \tag{2.6}$$

where $u \in L^2(\Omega)$. $H^k(\Omega)$ is defined as the set of functions such that itself and all its derivatives up to order k are in $L^2(\Omega)$.

The formulation of the weak form of the problem involves the definition of four collections of functions: the test functions and the trial solution functions, for the velocity field and for the pressure field. The space of velocity trial functions is denoted by S. This collection of functions consists of all functions which are square–integrable, have square integrable first derivatives over the computational domain Ω and satisfy the Dirichlet boundary conditions on Γ_D. This collection is defined as:

$$S = \{u \in H^1(\Omega) \mid u = u_D on \Gamma_D\} \tag{2.7}$$

This space contains vector functions such that each component is in the corresponding space of scalar functions.

The test functions for velocity belong to space ν. Functions in this class have the same characteristics as those in S, except that they are required to vanish in Γ_D where the velocity is prescribed. Space ν is defined as:

$$\nu = \{v \in H^1(\Omega) \mid v = 0 on \Gamma_D\} \tag{2.8}$$

Similarly, a space of function called Q is defined for the pressure. Since the space derivatives of pressure do not appear in the weak form of the Stokes problem, the functions in Q are simply required to be square integrable:

$$Q = \{q \in L^2(\Omega)\} \tag{2.9}$$

This space is both the trial space and the test function space. In the case of a purely Dirichlet velocity boundary condition, the pressure is defined up to a constant, and its value must be prescribed at one point of the domain Ω.

It follows that a function belonging to H^1 can be written as a linear combination of nodal basis functions N:

$$\phi^h = \sum_i \phi_i N_i \tag{2.10}$$

Be u^h the trial solution for velocity and p^h the trial function for pressure:

$$u^h = \sum_{i=1} u_i N_i^u \tag{2.11}$$

$$p^h = \sum_{i=1} p_i N_i^p, \tag{2.12}$$

Where N^u and N^p are the chosen interpolation function for the velocity and the pressure respectively. The fact that the velocity space and the pressure space are approximated independently leads to the nomenclature mixed formulation. In order to obtain the weak formulation, the momentum equations are weighted by a test function v^h and the continuity equation by a test function q^h. A finite element formulation is said to be Galerkin formulation if the trial (S_p^h, S_u^h) and test spaces (V_p^h, V_u^h) are the same up to the Dirichlet boundary conditions:

$$S_p^h := L_2(\Omega) \tag{2.13}$$

$$S_u^h := \{u^h \in H^1(\Omega) \mid u^h = \bar{u}\} on \partial\Omega_D \tag{2.14}$$

$$V_p^h := L_2(\Omega) \tag{2.15}$$

$$S_u^h := \{u^h \in H^1(\Omega) \mid u^h = 0\} on \partial\Omega_D \tag{2.16}$$

The standard discrete weak formulation for the Navier Stokes equations can be written as:

Find $(u^h, p^h) \in S_u^h \times S_p^h$ such that for all $(v^h, q^h) \in V_u^h \times V_p^h$:

$$\int_\Omega (\partial_t u^h) \cdot v^h dv + \int_\Omega (u^h \cdot \nabla u^h) \cdot v^h dv + \nu \int_\Omega \nabla u^h : \nabla v^h dv - \int_\Omega p^h (\nabla \cdot v^h) dv$$

$$= \int_{\Omega} f \cdot v^h dv + \int_{\partial\Omega_N} t \cdot v^h ds + \int_{\Omega} q^h (\nabla \cdot u^h) dv \tag{2.17}$$

From a linear algebra perspective, the Galerkin method leads to the following system by considering an implicit time discretization, here, backward Euler):

$$\begin{bmatrix} \frac{M^{n+1}}{\Delta t} + K^{n+1} + C^{n+1} & G^{n+1} \\ G^{Tn+1} & 0 \end{bmatrix} \begin{bmatrix} u^{n+1} \\ p^{n+1} \end{bmatrix} = \begin{bmatrix} f^{n+1} + \frac{M^{n+1}}{\Delta t} u^n \\ 0 \end{bmatrix} \tag{2.18}$$

Where u and p are the arrays of nodal velocities and pressures. M, K and C are mass, advective and convective matrix respectively. f is the body force. The above defined matrices are given as:

$$K = \int_{\Omega} B^T \nu B dV \tag{2.19}$$

$$C = \int_{\Omega} N^u u^h . \nabla N^u dV \tag{2.20}$$

$$G = \int_{\Omega} N^p \rho (\nabla N^u) dV \tag{2.21}$$

$$f = \int_{\Omega} N^u \rho g dV \tag{2.22}$$

Where the gradient matrix, B is defined as:

$$B_i = \begin{bmatrix} \frac{\partial N_i}{\partial x_1} & 0 \\ 0 & \frac{\partial N_i}{\partial x_2} \\ \frac{\partial N_i}{\partial x_1} & \frac{\partial N_i}{\partial x_2} \end{bmatrix} \tag{2.23}$$

Chapter 3

Multiphase Flow

3.1 Numerical Difficulties

There are some difficulties associated with the computation of two phase flow problems.

The first one is defining the accurate representation of the interface that seperates the two fluids. There are several techniques in this case with their own advantages and disadvantages.

Another numerical difficulty is originates from the fact that certain quantities may be discontinuous across the interface, e.g, density, viscosity and pressure. The simplest and most accurate technique to overcome this problem, is to regularize all jumps. The density and viscosity can be regularize such that instead of jumping discontinuously, they go smoothly from ρ_1 to ρ_2 over several grid points. However, it is shown that this smoothing approach introduces non-physical parameters leading to thermodynamical aberrations [6].

Recently, some techniques have been introduced to impose sharp discontinuities at the interface. Those techniques mainly rely on the partition of unity concept where the knowledge of the discontinuies is introduced in the approximation space. A popular example in the finite element community is the Extended Finite Element Method (XFEM) [7], in the finite difference context is the Ghost Fluid Method [8] and in the finite volume approach is the in-cell reconstruction technique [9].

3.2 Numerical Methods for Modelling Interface

Numerous techniques have been developed for incompressible two phase flow. The main difference between the method is how the interface is represented. The way that curvature and normal are calculated will naturally depend on the representation.

All interfaces representing Methods can be divided into two classes: interface capturing (IC) and ihnterface tracking (IT) metods. In the first class, the interface, Γ is represented implicitly by a function defined on all the domain.This class includes the Level Set method (LS) and the Volume Of Fluid method (VOF). In the second class, the interface, Γ is explicitly tracked. Among the front tracking methods, Marker Particles (MP) method, the Moving Mesh (MM) methods and the Gridless Methods (GM) are the most popular.

A short summary of the basic features of these methods is given in 3.1.

3.3 The Level Set Method

Flow problems are naturally described in an Eulerian framework where the computational mesh is fixed and the fluid moves with respect to the grid. The Eulerian formulation facilitates the treatment of large distortions in the fluid motion. Its drawback is the difficulty to follow interfaces between different materials. In an Eulerian description the finite element mesh is thus fixed and the continuum moves and deforms with respect to the computational mesh. As the material flows over the mesh, the physical properties of one element (for example its density or viscosity) will change through time due to material advection.

Level set methods are computational techniques for tracking moving interfaces; they rely on an implicit representation of the interface. Since the introduction of the level set method by Osher and Sethian [10], a large amount of bibliography on the subject has been published. See, for instance, the cited review by Sethian and Smereka [11] and the work by Osher and Fedkiw [12]. Level set methods are particularly designed for problems in multiple space dimensions in which the topology of the evolving interface changes during the course of events. This technique is commonly used in engineering problems to track interfaces location [13], [14] and cracks [15],[16]. It is also used in computational geometry applications, in grid generations, computer vision and other applications.

Table 3.1: Summary of techniques for interface computation: advantages and disadvantages

Method	Advantages	Disadvantages
VOF	Conceptually simple Good mass conservation	Complex interface reconstruction
LS	Conceptually simple Easy to implement Automatic topological changes	Poor mass conservation
MP	Extremely accurate Sharp interface	Mapping of interface mesh onto Eulerian mesh Manual breaking and merging Remeshing if large deformation
MM	Extremely accurate	Remeshing if large deformation Mesh motion difficult/costly in 3D
GM	Automatic topological changes	Expensive in 3D Boundary conditions

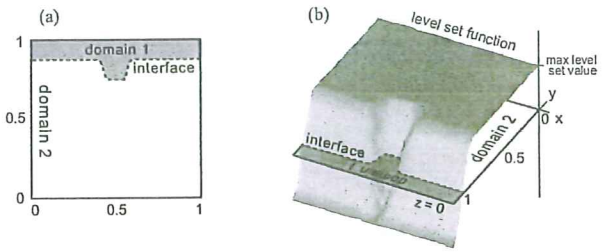

Figure 3.1: (a) The two materials are associated with thesign of the level set function. The dotted line is the interface. (b) Surface representation of the level set function.

The level set technique describes the location of the interface between materials by means of a function ϕ, called level set function, defined on the simulation domain. The sign of the level set function defines two geometrical domains using the following convention:

$$\phi(X,t) = \{ \begin{array}{ll} \geq 0 & \text{for x in domain 1} \\ = 0 & \text{for x on the interface} \\ \leq 0 & \text{for x in domain 2} \end{array} \tag{3.1}$$

where x stands for a point in the simulation domain and t is the time. The interface location is the set of points where the level set field vanishes (Fig.3.1). The material corresponding to each point of the simulation domain is thus determined by the sign of the level set function.

Initially, ϕ is set as a signed distance to the interface. Far enough from the interface, ϕ is truncated by maximum and minimum cutoff values. The resulting level set function describes the position of the interface independently of the computational mesh.

In the practical implementation, ϕ is described (interpolated) with the finite element mesh, and therefore the resolution of the approximated interface depends on the quality of this mesh. Usually the same mesh of the mechanical problem is used to describe the level set function. This is a reasonable approach; same resolution is obtained in describing interfaces and velocities used to update these interfaces.

The level set represents interfaces which do not necessarily coincide with the element edges. Thus, the same mesh can be used throughout the entire simulation to describe the interface. Mesh adaptivity is allowed for element concentration in the places where they are needed, while leaving coarse elements in less compromised areas. To locate phases, smaller elements close to the level set are allowed for an accurate description of the interface. As the level set function evolves, remeshing is needed to update the fine part of the mesh following the interface.

The level set ϕ is a material property and consequently it is transported by the velocity. Therefore, it is updated by solving the following pure advection equation (first order hyperbolic)

$$\phi_t + u \cdot \nabla\phi = 0 \tag{3.2}$$

where u is the velocity field computed by solving the Navier Stokes problem and ϕ_t the time derivative of the level set function. In this context, the velocity field is known in all the points of the domain. Thus, the level set is transported integrating equation 3.2 using an explicit timemarching scheme designed for the pure advective problem: the twostep third order Taylor Galerkin method [17], [18]. This method is straightforwardly implemented and computationally affordable. In similar situations other authors use the HamiltonJacobi equation to transport the interface. This is specially appropriate if the only available data is the front velocity, or if the velocity depends on the front itself, for example on its curvature. In the present situation the velocity is known everywhere as a vector and it is possible to directly integrate the pure advection problem. In general, the time evolution of the level set function is such that it does not conserve the property of being a truncated distance to the interface (as set for the initial configuration). However, for the current application this method is sufficiently accurate and it does not require any postprocess to reconstruct the distance shape.

The level set approach may describe changes in the shape (topology) of the phases. In practice, this allows the representation of detaching drops, merging bubbles, breaking sets, etc. This feature of the level set method is of great interest when used in some geophysical situations, for example to model slab breakoff, delamination, or any other process involving changes in the topology of the interface.

The description of the materials location given by the level set function is not

only useful for the mechanical problem, but it is also used in solving the Eulerian multiphase thermal equation.

3.4 Space discretization

The level set is discretized in space using a linear interpolation

$$\phi(X,t) \simeq \phi^h(X,t) = \sum_{i \in \mathcal{N}_{lin}} N_i(X)\phi_i(t) = N_T \Phi \tag{3.3}$$

where

$$\Phi = [\phi_1, \phi_2, ..., \phi_{nlin}] \tag{3.4}$$

The transport equation of the level set 3.2 is discretized using 3.3 and yields

$$M_\Phi \dot{\Phi} - G_\phi \Phi = 0 \tag{3.5}$$

Where;

$$M_\phi = \int_\Omega N_T^T N_T dV \tag{3.6}$$

$$G_\phi = -\int_\Omega N_T^T u^T (\nabla N_T) dV \tag{3.7}$$

3.5 Time discretization

The level set function is updated at each time step by the transport equation 3.2,which can be rewritten as

$$\dot{\phi} = -u \cdot \nabla \phi \tag{3.8}$$

This equation is integrated upon time using a twostep thirdorder TaylorGalerkin method (2STG3), namely

$$\tilde{\phi}^n = \phi^n + \frac{1}{3}\Delta t\dot{\phi}^n + \alpha\Delta t^2\ddot{\phi}^n \tag{3.9}$$

$$\phi^{n+1} = \phi^n + \Delta t\dot{\phi}^n + \frac{1}{2}\Delta t^2\tilde{\ddot{\phi}}^n \tag{3.10}$$

The α parameter takes the value $frac19$ to reproduce the phasespeed characteristics of the singlestep TaylorGalerkin scheme [18]. Taking into account the incompressibility equation 2.2, the second time derivative of the level set function ϕ can be expressed as

$$\ddot{\phi} = -u\cdot\nabla\dot{\phi} = u.\nabla(u\cdot\nabla\phi) = \nabla((u\cdot u)\nabla\phi) \tag{3.11}$$

therefore, the first step of the TaylorGalerkin algorithm is given by

$$\tilde{\phi}^n = \phi^n + \frac{1}{3}\Delta t(-u\cdot\nabla\phi^n) + \alpha\Delta t^2\nabla\cdot((u\cdot u)\nabla\phi^n) \tag{3.12}$$

Using the space discretization Φ of the level set function ϕ, the first and second steps of the TG3 scheme are expressed in the following matrix forms

$$M_\phi\tilde{\phi}^n = \left[M_\phi + frac13\Delta tG_\phi + \alpha\Delta t^2K_\phi\right]\Phi^n \tag{3.13}$$

$$M_\phi\phi^{n+1} = \left[M_\phi + \Delta tG_\phi\right]\Phi^n + \frac{1}{2}\Delta t^2K_\phi\tilde{\Phi}^n \tag{3.14}$$

where M_ϕ and G_ϕ are defined in 3.6 and 3.7, and K_ϕ comes from the discretization of the last term of 3.12

$$K_\phi = -\int_\Omega (u\cdot u)(\nabla N_T^T\nabla N_T)dV \tag{3.15}$$

Note that G_ϕ and K_ϕ depend on the velocity field. In the practical implementation, the velocity field u^n of the n step is taken constant during the entire time step and consequently the steady (quasistatic) Stokes problem is not solved for the

intermediate step $\tilde{\phi}^n$

To keep the solution in the stability domain of the 2STG3 algorithm the time increment Δt must be such that Courant vector (c_x, c_y) satisfy

$$c_x^2 + c_y^2 \leq \frac{3}{4} \tag{3.16}$$

where $c_x = u_x \frac{\Delta t}{h_x}$, $c_y = u_y \frac{\Delta t}{h_y}$ and h_i is the mesh size along the ith Cartesian direction. Thus, at most temporal steps the time increment Δt is set to satisfy 3.17

$$c_x^2 + c_y^2 = \frac{3}{4\theta} \tag{3.17}$$

with $\theta = 0.9$, That means that at each time step each particle moves approximately nine tenths of the size of the smallest element of the mesh. Nevertheless, there are situations in which this time increment is too large: if the velocity is slowing down to zero, in order to satisfy 3.17 the time increment grows to infinite. To avoid immense time increments, the criterion 3.13 and 3.14 is combined with a time increment for the diffusive part of the problem

$$\Delta t_{diff} = \frac{\theta h^2}{2k} \tag{3.18}$$

where k is the thermal diffusivity and h, the size of an element.

3.6 Enriched Solution (XFEM)

The level set method is usually combined with an enrichment technique to improve the accuracy of the solution in the vicinity the interface. The combination of finite element with these two numerical techniques is called eXtended Finite Element Method (XFEM) [19]. XFEM is particularly suitable for multiphase problems in which the strain rate is discontinuous across the interface due to the continuity of stress and a step in the viscosity.

The enrichment technique used here adds dynamically some degrees of freedom to the mechanical solution to catch the discontinuity exactly where it is expected to

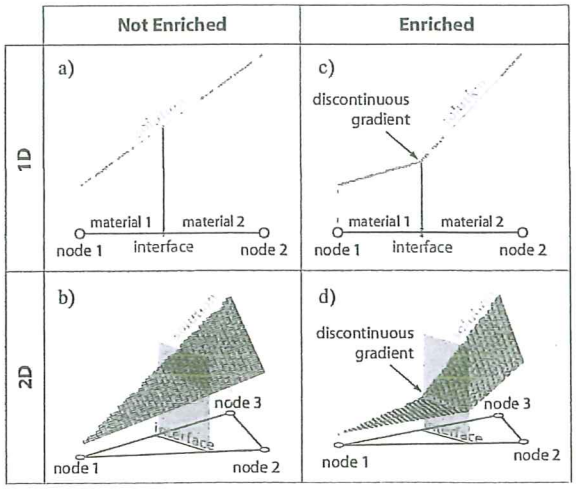

Figure 3.2: Discontinuous gradient is obtained using enrichment. The velocity gradient (strain rate) will be discontinuous across the interface, caused by the continuity of stress and the step in the viscosity.

happen, i.e. over the interface described by the level set.

The enrichment improves the solution near the interface described by the level set. Fig.3.2 shows how the enrichment technique modifies the solution inside multiphase elements.

The mixed formulation of the Stokes problem uses different interpolations for velocity u and pressure p. The minielement, shown in (Fig.2.1), determines these interpolation spaces. Denoting by $\mathcal{N}_{lin}$ the indices associated with the vertex nodes and $\mathcal{N}_j$, for $j \in \mathcal{N}_{lin}$, the corresponding shape functions, the interpolated pressure is:

$$p(x,t) \simeq p_h(x,t) = \sum_{j \in \mathcal{N}_{lin}} N_j(x) P_j(t) \tag{3.19}$$

The interpolation of the velocity also includes the bubble degrees of freedom N_j for $j \in \mathcal{N}_{bub}$, namely:

$$u(x,t) \simeq u_h(x,t) = \sum_{j \in \mathcal{N}_{lin} \cup \mathcal{N}_{bub}} N_j(x) u_j(t) \tag{3.20}$$

The level set formulation is interpolated in terms of the linear degrees of freedom:

$$\phi(x,t) \simeq \phi_h(x,t) = \sum_{j \in \mathcal{N}_{lin}} N_j(x) \phi_j(t) \tag{3.21}$$

In order to improve the ability of the interpolation to represent the gradient discontinuities across the interface, the interpolation of the velocity and pressure are enriched using a partition of the unity approach and a ridge function R, defined as [14]:

$$R(x) = \sum_{j \in \mathcal{N}_{enr}} \mid \phi_j \mid N_j(x) - \mid \sum_{j \in \mathcal{N}_{enr}} \phi_j N_j(x) \mid \tag{3.22}$$

Note that R is defined such that it is only different from zero in the elements containing part of the interface. The enrichment affects only the degrees of freedom corresponding to the vertex nodes of the elements in contact with the interface. The set of indices corresponding to such nodes is denoted as $\mathcal{N}_{enr}$. Thus enriched interpolations of velocity and pressure are expressed as:

$$u_h(x,t) = \sum_{j \in \mathcal{N}_{lin} \cup \mathcal{N}_{bub}} N_j(x) u_j(t) + \sum_{j \in \mathcal{N}_{enr}} M_j(x) a_j(t) \tag{3.23}$$

and,

$$p_h(x,t) = \sum_{j \in \mathcal{N}_{lin}} N_j(x) P_j(t) + \sum_{j \in \mathcal{N}_{enr}} M_j(x) b_j(t) \tag{3.24}$$

Where a_j and b_j are, respectively, the additional degrees of freedom for velocity and pressure and its associated interpolation function M is defined as

$$M_j(x) = R(x) N_j(x) \tag{3.25}$$

A compact matrix expression of the interpolation of velocity and pressure is used in the following:

Chapter 4

GLS Stabilization

4.1 GLS Formulation of Navier Stokes Equation

Stabilization approach applied to the Transient Navier Stokes equations is Galerkin-Least-Squares (GLS) method, in which a least-squares form of the element residual is added to the basic Galerkin equations.GLS formulation deals with convection and pressure stabilization. In this case, the main unknowns are approximated by the usual finite element components and an additional subgrid scale term which enhances stability of the resulting problem [20].

The transient Navier Stokes equations is recalled as:

$$\partial_t u + u \cdot \nabla u - \nu \Delta u + \nabla p = f \tag{4.1}$$

$$\nabla \cdot u = 0 \tag{4.2}$$

After integration by part the weak form of the problem is written as following in a space-time slab $\Omega \times]t_n, t_{n+1}[$. It consists of finding u and p, functions of space and time such that the following weak form is satisfied for all test functions v and q which are time dependant.

$$\int_{t^n}^{t^{n+1}} \int_{\Omega} [\partial_t u \cdot v + \nu \nabla u : \nabla v + (u \cdot \nabla u) \cdot v - p \nabla \cdot v + q \nabla \cdot u - f \cdot v] d\Omega dt$$

$$+ \int_{\Omega} [u(t_n^+) - u(t_n^-)] \cdot v d\Omega = 0 \tag{4.3}$$

u is assumed to be discontinuous between time slabs and, in particular, the notation involved in the last term of 4.2 is $u(t_n^{+,-}) = lim_{\varepsilon \to 0^{+,-}} u(t_n + \varepsilon)$. This term imposes weakly the continuity of the velocity at t_n (and the initial condition when $n = 0$). It is remarked that the momentum and the continuity equations are written as a single variational equation.

The discrete problem is obtained by approximation u and p. If u_h and p_h are the finite element unknowns, we approximate $u \approx u_h + \tilde{u}$ and $p \approx p_h$, that is, the velocity is approximated by its finite element component plus an additional term that we call subgrid scale or subscale.

The velocity and pressure interpolation in time are assumed as piecewise constant. Velocity in the time interval $]t_n, t_{n+1}[$ is defined as:

$$u^{n+1} \approx u_{n+1}^* := u_h^{n+1} + \tilde{u}^{n+1} \tag{4.4}$$

And pressure in the time interval $]t_n, t_{n+1}[$ is defined as:

$$p^{n+1} \approx p_h^{n+1} \tag{4.5}$$

In which u_h^{n+1} and p_h^{n+1} are obtained using the standard finite element interpolation. In particular, equal velocity-pressure interpolation is possible with the formulation to be derived.

If in 4.3 u is replaced by $u_*^{n+1} := u_h^{n+1} + \tilde{u}^{n+1}$, constant in $]t_n, t_{n+1}[$, and p is replaced by p_h^{n+1}, the terms involving $\tilde{u}^{n+1}$ are integrated by parts, and the test functions are taken in the finite element space (also constant in the time interval considered), one gets:

$$\begin{aligned} &\delta t \int_\Omega [\nu \nabla u_h^{n+1} : \nabla v_h + (u_*^{n+1}.\nabla u_h^{n+1}) \cdot v_h - p_h^{n+1} \nabla \cdot v_h \\ &+ q_h \nabla \cdot u_h^{n+1} - f^{n+1} \cdot v_h] d\Omega + \int_\Omega [u_*^{n+1} - u_*^n] \cdot v_h d\Omega \\ &\qquad - \delta t \int_\Omega \tilde{u}^{n+1} \cdot (\nu \Delta_h v_h + u_*^{n+1} \cdot \nabla v_h + \nabla q_h) d\Omega = 0 \end{aligned} \tag{4.6}$$

Where notation Δ_h is used to indicate that the Laplacian needs to be evaluated element by element and f^{n+1} needs to be understood as the average of f in $]t_n, t_{n+1}[$.

Equation 4.6 must hold for all test functions v_h and q_h in their corresponding finite element spaces. It is important to note that the advection velocity in 4.6 is u_*^{n+1} and also that the continuity between time slabs needs to be imposed in terms of this velocity.

After deviding 4.6 by δt and integration by part over v_h, 4.7 will be yielded as following:

$$\int_\Omega [-\nu\Delta u_h^{n+1} \cdot v_h + u_*^{n+1} \cdot \nabla u_h^{n+1} v_h + \nabla p_h^{n+1} v_h - f^{n+1} \cdot v_h] d\Omega$$

$$+ \int_\Omega [\frac{1}{\delta t} u_*^{n+1} - u_*^n \cdot v_h - \Delta\tilde{u}^{n+1}\nu v_h + \nabla\tilde{u}^{n+1} \cdot u_*^{n+1} v_h] d\Omega = 0 \tag{4.7}$$

The equation 4.7 is rewritten as:

$$-\nu\Delta u_h^{n+1} + u_*^{n+1}.\nabla u_h^{n+1} + \nabla p_h^{n+1} - f^{n+1} + \frac{u_*^{n+1} - u_*^n}{\delta t}$$

$$-\nu\Delta\tilde{u}^{n+1} + \nabla\tilde{u}^{n+1} u_*^{n+1} = 0 \tag{4.8}$$

If we consider following assumption:

$$\delta_t u_*^n = \frac{u_*^{n+1} - u_*^n}{\delta t} \tag{4.9}$$

Equation 4.8 can be recalled as:

$$-\nu\Delta u_h^{n+1} + u_*^{n+1}.\nabla u_h^{n+1} + \nabla p_h^{n+1} - f^{n+1} + \delta_t u_*^n$$

$$-\nu\Delta\tilde{u}^{n+1} + \nabla\tilde{u}^{n+1} u_*^{n+1} = 0 \tag{4.10}$$

This equation states that u_*^{n+1}, p_h^{n+1} has to be solution of the Navier-Stokes equations within each element taking account a piecewise constant time interpolation.

Our intention here is to recover a well-known GLS-type formulation, and for this we need to make two additional assumptions. The first one is to take advection velocity, u_h^{n+1} instead of u_*^{n+1}. and the second one is to neglect $\delta_t u_*^n$.

Residual, R_h^{n+1} is defined as 4.11. By considering 4.11, 4.10 is rewritten to 4.12:

$$-\nu\Delta\tilde{u} + u_h^{n+1}.\nabla\tilde{u}^{n+1} = -R_h \tag{4.11}$$

$$\tau_{gls}[f^{n+1} - (-\nu\Delta u_h^{n+1} + u_h^{n+1}.\nabla u_h^{n+1} + \nabla p_h^{n+1})] = -\tau_{gls}R_h^{n+1} \tag{4.12}$$

Where τ_{gls} is a numerical parameter for which an expression is proposed in the next section and R_h^{n+1} is the residual defined for Navier Stokes equation evaluated with u_h^{n+1}.

4.2 Extra Stablized Matrices

Considering all approximation, the final discrete problem to be solved for u_h^{n+1} and $p^{n+1}h$ is:

$$\int_\Omega [\tfrac{1}{\partial t}(u_h^{n+1} - u_h^n) \cdot v_h + \nu\nabla u_h^{n+1} : \nabla v_h + (u_h^{n+1} \cdot \nabla u_h^{n+1}) \cdot v_h - p_h^{n+1}\nabla \cdot v_h$$

$$+\tau_{gls}(\nu\Delta_h v_h + u_h^{n+1} \cdot \nabla v_h) \cdot R_h^{n+1} - f^{n+1} \cdot v_h]d\Omega = 0 \tag{4.13}$$

$$\int_\Omega [q_h\nabla \cdot u_h^{n+1} + \tau_{gls}\nabla q_h \cdot R_h^{n+1}]d\Omega = 0 \tag{4.14}$$

From the above equation extra matrices, K_h, γ and $\bar{f}$ which must be added to K, G and the source term respectively, are obtained as:

$$K_h = \tau_{gls}\int_\Omega u_h^{n+1} \cdot \nabla N^u u_h^{n+1} \cdot \nabla N^u dV \tag{4.15}$$

$$\gamma = \tau_{gls}\int_\Omega u_h^{n+1} \cdot (\nabla N^u \nabla N^p)dV \tag{4.16}$$

$$\bar{f} = \rho g\int_\Omega u_h^{n+1} \cdot \nabla N^u dV \tag{4.17}$$

Final stabilized system for obtaining stabilized pressure and velocity is as following:

$$\begin{bmatrix} \frac{M^{n+1}}{\Delta t} + K^{n+1} + C^{n+1} + K_h^{n+1} & G^{n+1} + \gamma^{n+1} \\ G^{Tn+1} + \gamma^{Tn+1} & 0 \end{bmatrix} \begin{bmatrix} u^{n+1} \\ p^{n+1} \end{bmatrix} = \begin{bmatrix} f^{n+1} + \bar{f}^{n+1} + \frac{M^{n+1}}{\Delta t} u^n \\ 0 \end{bmatrix} \tag{4.18}$$

4.3 GLS Stabilization Factor

In order to obtain stabilization factor, τ, the left hand side of the following equation is considered separately:

$$-\nu \Delta u + u.\nabla u = -R_h \tag{4.19}$$

as:

$$-\nu \Delta u = -R_h \tag{4.20}$$

and:

$$u.\nabla u = -R_h \tag{4.21}$$

At first we start with 4.20. If we assume u as a polynomial as:

$$u = a_0 + a_1 x + a_2 x^2 \tag{4.22}$$

Then,

$$\Delta u = 2a_2 \tag{4.23}$$

after applying 4.23 in 4.20:

$$2a_2 = \frac{R_h}{\nu} \tag{4.24}$$

After replacing 4.24 in 4.22:

$$u(x) = \frac{R_h}{2\nu} x(h - x) \tag{4.25}$$

x is assumed as center of the interval for linear interpolation. So, it is equivalent to $\frac{h}{2}$ and 4.25 is rewritten as:

$$u(x) = \frac{R_h}{2\nu} \frac{h^2}{4} \tag{4.26}$$

The second step is to consider 4.21. In the same way by assuming velocity as a polynomial function as it is defined in 4.22, 4.21 will be yield as:

$$u(x) = \frac{R_h}{\mid u \mid} x \tag{4.27}$$

As it has been assumed before, x is equivalent to $\frac{h}{2}$. So, 4.27 is yielded as:

$$u(x) = \frac{R_h}{\mid u \mid} \frac{h}{2} \tag{4.28}$$

According to what is obtained in 4.26 and 4.28 and also what is obtained before as $u(x) = \tau_{gls} R_h(x)$, τ_{gls}, the stablization factor is obtained as:

$$\tau_g ls = \left[(\frac{\nu}{8h^2})^2 + (\frac{\mid u \mid}{2h})^2 \right]^{-\frac{1}{2}} \tag{4.29}$$

Chapter 5

Results

5.1 Rayleigh-Taylor Instability

In order to prove the numerical method used in the current code, a typical benchmark for two phase flow, Rayleigh Taylor instability has been used. In this case, the same values of viscosity of 0.00313 $kgm^{-1}s^{-1}$ has been considered for both fluids. Densities of 1.225 and 0.1694 Kgm^{-3} for the upper and downer fluids respectively. A 1 m wide, 1.5 m height rectangular domain has been discretized using different grid sizes which will be explained in the following sections.

The initial level set is defined as a cosine function,$c = \frac{1}{20}cos(2\pi x) + 0.7$. The initial velocity field is zero, pressure field is hydrostatic. No-slip boundary condition has been imposed on the bottom wall ans slip boundary condition on the side walls. A prescribed zero pressure has been applied to the upper wall.

The abofve mentioned physical properties of viscosity and densities are defined so that the obtained results will be comparable with those of available numerical results of our case [21].

5.2 Convergence criteria

Since convective term is the nonlinear part of the equation and convective matrix has been calculated according to the prescribed velocity, an iterative scheme is needed to be defined in order to reach to the solution.

Two different criteria has been taken account for convergence: Residual convergence and velocity convergence.

In the first case, the residual value is calculated after each solution as:

$$Residual = [f] + \frac{[M][u]^1}{dt} - ([K][C_v]\frac{M}{dt})[u]^1 - [G]^T[P]^1 \tag{5.1}$$

in which $[u]^1$ and $[P]^1$ are prescribed velocity and pressure vectors in the first iteration and previous velocity and pressure in the next iteration. The relative value of residual is considered as convergence parameter in iterative scheme:

$$Relative - Residual = \frac{\parallel [Residual] \parallel}{\parallel ([f] + \frac{[M][u]^1}{dt}) \parallel} \tag{5.2}$$

Velocity error has been defined relatively as another parameter of convergence in iterative scheme. In which $[u]^2$ and $[u]^1$ are two consequative velocity vectors in each iteration.

$$Relative - Error = \frac{(([u]^2 - [u]^1)[K]([u]^2 - [u]^1)^T)}{[u]^2[K][u]^{2^T}} \tag{5.3}$$

In each time step, the iretative scheme is going on until both defined values in 5.2 and 5.3 decreased to the tolerance value assumed as 0.001 or limited iteration number of 50 is satisfied.

5.3 Transient Navier Stokes without enrichment

The following simulations illustrate the results which have been obtained based on transient navier stokes solution without enrichment, in a discretized domain using grid size of 30×45. The material propertise have been selected as described in 5.1.

The obtained results are not in good agreement with those of [21]. There is no vortice visualized in our simulation while vortices started to be constructed after time 0.7 sec in the mentioned work. Assuming surface tension equal to zero can justify this phenomena.

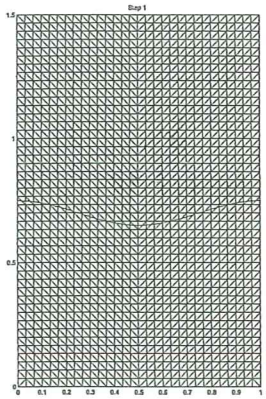

Figure 5.1: Rayleigh-Taylor Instability at first time step; grid size of 30×45

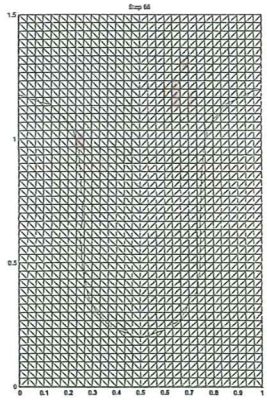

Figure 5.2: Rayleigh-Taylor Instability at time step 66; grid size of 30×45

However, some results have been obtained with different values of viscosity and density (viscosity values of 0.8 and 0.5 $kgm^{-1}s^{-1}$ and density values of 100 and 50 Kgm^{-3}) which include vortices. Fig. 5.3, 5.4, 5.5, 5.6 and 5.7 illustrate Rayleigh-Taylor instability at different time steps. Fig. 5.8 is brought [21] as a sample though the physical properties are not the same.

Fig.5.9 and Fig.5.10 illustrate residual and velocity convergence related to illustrated simulation of Fig.5.2. These graphs prove the numerical method has been applied in the code.

5.4 Volume conservation

The volume of each phase is expected to remain unchanged along the time stepping procedure due to conservative equation. Therfore, volumetric changes in time can be used to assess the accuracy of the numerical techniques.

As illustrated in 5.1, the finer the mesh, the better description of the level set, hence, less volume variation is observed. Even with a coarse mesh small error has been produced.

5.5 Lack of Symmetry

In this work, the mesh arrangement is completely symmetric. So, it is expected to have symmetric results. But the results are not symmetric. At first glance, one may think it comes from selected time integration method.

In order to check this possibility, an error has been defined as 5.4 In which $[V]$ is the obtained velocity vector and $[V_{sym}]$ is a vector with the same size as velocity vector with the components equal to unit value exept on the boundries and symmetry line which are replaced by zero. n is number of nodes. In order to eliminate the nonlinearity error, the convective matrix has been removed.

$$symError = \frac{[V][V_{sym}]}{n} \tag{5.4}$$

As it is illustrated in Fig.5.11, the value of error is increasing along time stepping procedure but decreases by refining the mesh. It can be concluded that this error is

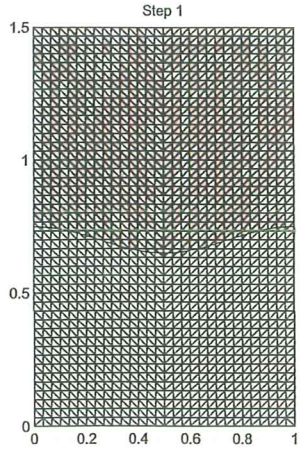

Figure 5.3: Rayleigh-Taylor instability: Grid size 30 × 45 at time 0.01

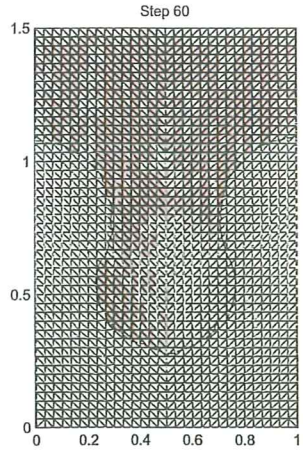

Figure 5.4: Rayleigh-Taylor instability: Grid size 30 × 45 at time 0.6

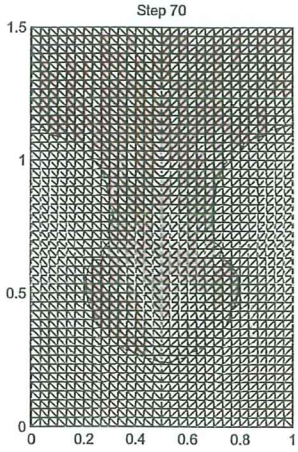

Figure 5.5: Rayleigh-Taylor instability: Grid size 30 × 45 at time 0.7

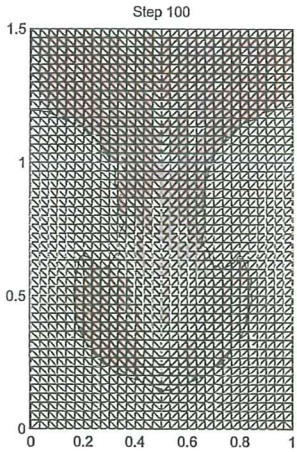

Figure 5.6: Rayleigh-Taylor instability: Grid size 30 × 45 at time 1.0

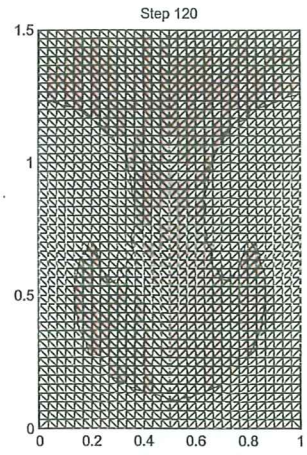

Figure 5.7: Rayleigh-Taylor instability: Grid size 30 × 45 at time 1.2

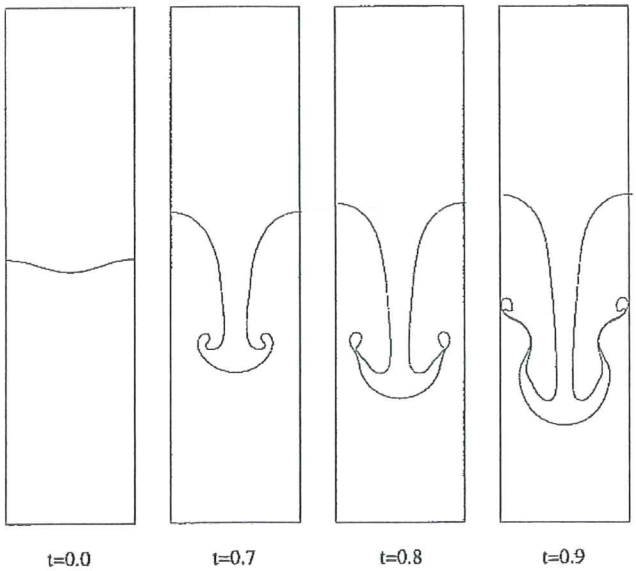

Figure 5.8: Rayleigh-Taylor instability on a 64 × 256 grid size using the front-tracking algorithm [21]

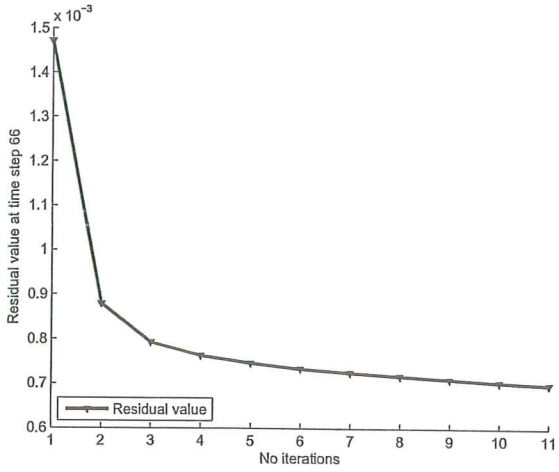

Figure 5.9: Residual convergence at time step 66

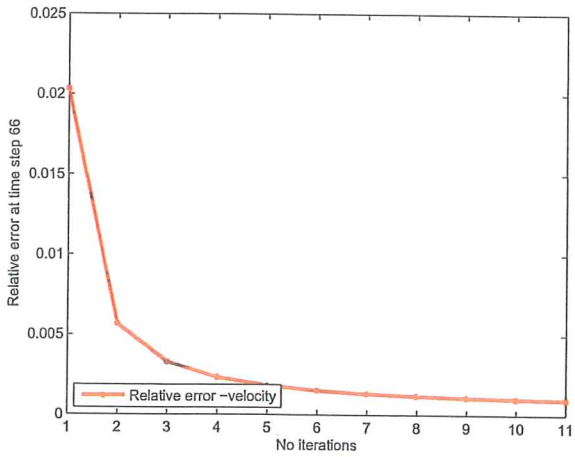

Figure 5.10: Velocity convergence at time step 66

Table 5.1: Maximum volume variation on different grid size along time stepping procedure

Grid size	Initial Volume of Denser Fluid	Δ Vol	Error
30×45	0.8	0.0037	% 0.47
40×60	0.8	0.0032	% 0.4
50×75	0.8	0.002	% 0.25

coming from time integration method and can be overcome by refining the mesh.

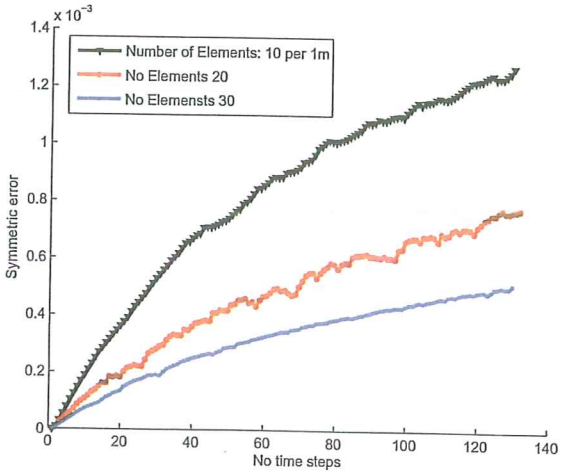

Figure 5.11: Symmetry error

Chapter 6

Conclusion

Presented results in Chapter 5 shows that the implemented code based on FEM and level set method has the ability of modelling multiphase transient Navier Stokes equations with high accuracy. Although the code has been implemented for stabilized case and non stabilized one with enrichment convergence did not obtained. There are some points to be mentioned for future work:

Surface tension has been assumed zero in the current code. It can be added to the equation in order to have better results specially in Rayleigh-Taylor instability case.

The deficiencies of implememnted code including enrichment and stablized equation has to be removed in order to get comparative results with non enriched transient Navier Stokes equation.

Tank sloshing can be modelled as another bench mark to verify the code specially in high contrasts of density and viscosity.

Bibliography

[1] Emilie Marchandise. Simulation of three dimensional two phase flows. *Universite Catholique de Louvain*, 2006.

[2] L. Moresi. S. Zhong and M. Gurnis. The accuracy of finite element solutions of stokes flow with strongly varying viscosity. *Phys. Earth Planet. Inter.*, 97:8394, 1996.

[3] A. Ladyzhenskaya. The mathematical theory of viscous incompressible flow. *Gordon and Breach Science*, 1969.

[4] Babuska. Error-bounds for finite element method. *Num. Math.*, 16:322333, 1970.

[5] Brezzi. On the existence, uniqueness and approximation of saddle- point problems arising from lagrangian multipliers. *RAIRO Anal Numer*, 8(R2):129151, 1974.

[6] J.H Ferziger. Interfacial transfer in tryggvason's method. *International Journal for Numerical Methods in Fluids*, 41(5):551–560, 2003.

[7] Chessa and T. Belytschko. An extended finite element method for two-phase fluids. *Journal of Applied Mechanics Transaction of ASME*, 70:10–17, 2003.

[8] M. Kang. R. Fedkiw. and X.-D Liu. A boundary condition capturing method for multiphase incompressible flow. *SIAM Journal on Scientific Computing*, 15:323–360, 2000.

[9] V. Smiljanovski. V. Moser and R. Klein. A capturing/tracking hybrid scheme for deflagration discontinuities. *Combustion Theory and Modelling*, 1:183–215, 1997.

[10] S. Osher and J. A. Sethian. Front propagating with curvature dependent speed: algorithms based on hamilton-jacobi formulations. *Journal of Computational Physics*, 79:1249, 1988.

[11] J. A. Sethian and P. Smereka. Level set methods for fluid interfaces. *Annual Review of Fluid Mechanics*, 35:341372, 2003.

[12] S. Osher. and R. Fedkiw. Level set methods: an overview and some recent results. *Journal of Computational Physics*, 169:463502, 2001.

[13] J. Chessa and T. Belytschko. An extended finite element method for twophase fluids. *Transactions of the ASME*, page 1017, 2003.

[14] N. Moes. M. Cloirec. P. Cartaud. and J. F. Remacle. A computational approach to handle complex microstructure geometries. *Comput. Methods Appl. Mech. Engrg.*, 192:31633177, 2003.

[15] T. Belytschko and T. Black. Elastic crack growth in finite elements with minimal remeshing. *International Journal for Numerical Methods in Engineering*, 45(5):601620, 1999.

[16] M. Stolarska. D. L. Chopp. N. Mos. and T. Belytschko. Modelling crack growth by level set in the extended finite element method. *Numerical Methods in Engineering*, 51:943960, 2001.

[17] V. Selmin. Thirdorder finite element schemes for the solution of hyperbolic problems. *Technical report, INRIA*, 1987.

[18] J. Donea. and A. Huerta. Finite element methods for flow problems. *Wiley Chichester West Sussex PO19 8SQ*, 2002.

[19] Sergio Zlotnik. Pedro Diez. Manel Fernandez. Jaume Verges. Numerical modelling of tectonic plates subduction using x-fem. *Computer methods in applied mechanics and engineering*, 196:4283–4293, 2007.

[20] Hughes TJR. Feijoo GR. Mazzei L. Quincy JB. The variational multiscale method -a paradigm for computational mechanics. *Computer Methods in Applied Mechanics and Engineering*, 166:3–24, 1998.

[21] Stephane Popinet. Stephane Zaleski. A front-tracking for accurate representation of surface tension. *International Journal For Numerical Methods In Fluids*, 30:775–793, 1999.